Bulletin of the New Zealand Society for Earthquake Engineering, Vol. 55, No. 3, September 2022

DEVELOPMENT OF LSN-BASED PIPE REPAIR RATE MODELS UTILISING DATA FROM THE 2011 CHRISTCHURCH EARTHQUAKES

Jose M. Moratalla[1] and Vinod K. Sadashiva[2]

(Submitted *June 2021*; Reviewed *August 2021*; Accepted *January 2022*)

ABSTRACT

The Canterbury Earthquake Sequence (CES) adversely impacted built, economic and social environments. This included widespread physical damage to the water supply pipe network in Christchurch, resulting in long service disruptions. The transient and permanent ground deformations generated by the earthquakes in the CES caused a range of pipe damage, particularly in the M_W 6.2 22 February 2011 and the relatively less damaging M_W 6.0 13 June 2011 event. Damage to the pipes in both events was largely attributed to liquefaction and lateral spreading effects. Pipes made of ductile material (e.g. PVC, HDPE) sustained lesser damage (and therefore lower repair rates) compared to the pipes made of non-ductile material (e.g. AC, CI). In all cases, the repair rates (number of repairs per kilometre) typically increased with increasing liquefaction severity.

Utilising the pipe repair dataset and Liquefaction Severity Number (LSN) maps generated from extensive geotechnical investigation following the CES events, new repair rate prediction models for water pipes subjected to liquefaction effects have been derived and are presented in this paper. Repair data from both earthquakes has been analysed independently and in combination, providing two sets of repair rate functions and different levels of uncertainty. Repair rate functions were first derived from pipes grouped by combination of diameter (i.e. $\phi < 75$ mm or $\phi \geq 75$ mm) and material type (i.e. ductile or non-ductile). The models were then refined by adding correction factors for those material types and diameters with sufficient sample length. Correction factors were derived for AC, CI, PVC pipes of diameter ≥75 mm and for MDPE and HDPE80 pipes of diameter <75 mm. Galvanised Iron (GI) pipes performed poorly during the earthquakes, resulting in very high repair rates compared to the other non-ductile pipes of diameter <75 mm damaged in the network; this warranted a separate repair rate model to be developed for this pipe type. The proposed models can be used in risk assessment of water pipe networks; i.e. to estimate the number of pipe repairs from potential liquefaction damage from future earthquakes.

INTRODUCTION

Pipes are an integral part of water supply networks that are vulnerable to natural hazards such as earthquakes [1-6]. As extensively documented in the literature (e.g. [7,8]), Christchurch city and the surrounding areas were shaken by a series of strong earthquakes in the period between September 2010 and December 2011. This included the primary earthquake on 4th September 2010 (M_W 7.1 event), followed by major aftershocks such as the M_W 6.2 22nd February 2011 and the M_W 6.0 13th June 2011 earthquakes that caused significant and widespread damage to the city's land and built environment. A key characteristic associated with the February and June 2011 earthquakes was the strong shaking accompanied by widespread and severe liquefaction in many areas in Christchurch city. It was observed that the buried water pipes were generally subjected to transient ground deformations (TGD, induced by seismic wave propagation) and permanent ground deformations (PGD, mostly due to liquefaction effects such as large vertical and/or lateral ground displacements, cracks and fissures). These deformations were often above the capacity of the pipelines to sustain such movements/loads, thereby resulting in wide-spread and numerous pipe faults (i.e. leaks or breaks) due to rotation and/or axial compression in the pipeline bodies and joints [9,10]. Of the two types of deformations, PGDs significantly affected the pipes compared to the effect of TGDs [10,11] In this paper we focus on fragility model development based on data relating to water pipes damaged due to PGD (in particular, liquefaction effects represented by the Liquefaction Severity number, or LSN) from the 22nd February and 13th June 2011 earthquakes.

Empirical fragility models for pipes are typically in the form of pipe repair rate models, where Repair Rate (RR) is expressed as number of repairs per kilometre of pipeline exposed to the hazard. The severity of liquefaction effects can be represented using direct measures of the PGD (e.g. vertical settlements, angular distortions, lateral ground strains, etc.) or other parameters such as the Cone Penetration Test (CPT)-based liquefaction vulnerability parameters (e.g. Liquefaction Severity Number) [12].

Observed permanent ground deformations due to liquefaction effects have been used by several authors [13-20] to derive RR functions using damage data from historical earthquakes (see Table 1). In the CES events, pre- and post-event high-resolution Light Detection and Ranging (LiDAR) data were available; high-resolution measurements of the angular distortion (β) and lateral ground strains (εHP) after the 22 February 2011 and 13 June 2011 earthquakes were used by [10,21] to derive RR models. β is defined as the observed differential vertical movement between two adjacent points separated a defined distance, whereas εHP is the maximum absolute value of the ground strain. Due to the lack of predictive models for these direct displacement metrics, these models are not favourable for use in pipe damage modelling [11,22].

[1] *Corresponding Author, GNS Science, Lower Hutt, j.moratalla@gns.cri.nz (Member)*
[2] *Senior Risk Engineer, GNS Science, Lower Hutt, v.sadashiva@gns.cri.nz (Member)*

Table 1: Summary of studies that have proposed PGD-based Repair Rate (RR) models for water pipes. Complete names of the pipe materials are given in the list of acronyms.

Study Reference	PGD Measurement	Earthquakes Causing the Damage	Pipe Diameter (ϕ)	Pipe Materials	Functional Form of RR Model
[10]	Angular distortion (β) and/or Lateral ground strain (ε_{HP})	Christchurch CES (22 February 2011, 13 June 2011)	>75 mm	AC, CI, PVC	Linear
[13]	Ground settlement contours	1906 San Francisco 1989 Loma Prieta	Mains (100–450 mm)	CI, RI, S, WS, DI with rigid joints DI with flexible joints	Bi-linear
[14]	Observed differential settlement	1985 Michoacan, Mexico	122 cm	Undifferentiated	Bi-linear
[15,16]	None, partial and total liquefaction (as in [15])	1995 Hyogoken-nanbu, Kobe	>75 mm	DIP, CIP, VP, SP, ACP	Bi-linear
[18,19]	Observed vertical settlement, lateral spreading and tectonic uplift	1995 Hyogoken-nanbu (Kobe), 1994 Northridge, 1989 Loma Prieta, 1971 San Fernando	Mains (100–450 mm)	Generic (derived using AC, CI, WS, S, DI and PVC data)	Exponential
[20]	Observed PGD	Not defined	Not specified	Ductile (DI, S, PVC) and brittle (AC, CI, RCC)	Exponential
[21]	Angular distortion (β) and/or Lateral ground strain (ε_{HP})	Christchurch CES (22 February 2011)	>75 mm	AC, CI, PVC	Linear

Liquefaction triggering analysis methods [23-25] are commonly used to evaluate the potential of a saturated soil layer to be liquefied. The safety factor against liquefaction (FS_{liq}) is expressed as the ratio between the resistance of the soil against liquefaction (or Cyclic Resistance Ratio of the soil (CRR)) and the earthquake induced load, expressed in terms of cyclic shear stress (CSR):

$$FS_{liq} = \frac{CRR}{CSR} \quad (1)$$

CRR is calculated using the Cone Penetration Test (CPT) tip resistance and sleeve friction, corrected for effective overburden stress using an iterative procedure. CSR is function of the normal and effective overburden stress, the peak ground acceleration (PGA), and the magnitude scaling factor. According to the method, liquefaction can be expected to occur when FS<1.

Liquefaction Resistance Index (LRI; [26]), Liquefaction Potential Index (LPI; [27]), One-Dimensional Volumetric Reconsolidation Settlement (SV1D; [28]) and Liquefaction Severity Number (LSN; [28]) are all liquefaction vulnerability parameters that have been used to derive RR functions (Table 2). These parameters are based on the liquefaction triggering analysis methods [23-25] that require detailed information about the subsurface conditions; the complexity of the liquefaction phenomena makes these methods subjected to large uncertainties due the local variability in the lithological conditions [29]. A brief overview of the four parameters and their use in RR models is provided below.

LRI is a representation of the aggregated CRR of soil layers up to 3.5 m below ground surface, weighted by PGA and earthquake magnitude. This parameter has been exclusively used to characterise the CES earthquakes. For example, Cubrinovski et al. [30] defined five liquefaction severity zones in Christchurch and calculated the number of repairs per kilometre of pipeline within each zone for different materials. However, this study does not provide regression models or differentiate the pipe diameters used in the assessment. The same LRI zones were used by [31] to derive Peak Ground Velocity (PGV)-based RR functions for high, average and low performance grouped pipes, as well as separate functions for pipes made of specific materials. Liquefaction effects were also included in [31] study through correction factors for the CRR at the estimated ground water depth.

LPI was proposed by [27] to parametrise the expected severity of liquefaction. Its value ranges from 0 to around 100, covering from no to severe effects of liquefaction. The method to calculate LPI utilises the safety factor against liquefaction (FS, [23-25]) along with the liquefied layer thicknesses and depths.

SV1D ([28]) is an estimator of the expected vertical ground settlement of liquefaction at the surface level. It is calculated through the integration of the vertical volumetric strain of the soil layers below the ground surface. The analysis carried by [32] showed that SV1D is not a good predictor of ground subsidence but is recommended as an index of the expected liquefaction damage at the ground surface.

LSN ([28]) reflects how severe the effects of liquefaction are expected to be, and its value ranges from 0 (for no liquefaction effects) to a large value (e.g. 50 where extreme permanent ground deformations are expected). This parameter has been shown to correlate well with land and built infrastructure damage [28,32-35] and, in particular, with damage to buried water pipes [11,36,37]. It is calculated as the summation of the volumetric densification strain (εv) expected in the liquefiable layers up to 10 m soil depth (z), below the ground water table:

$$LSN = \int \frac{\varepsilon v}{z}\, dz \quad (2)$$

Here, εv is assessed from liquefaction triggering analysis [23-25], and it is function of the ground shaking level and the earthquake magnitude. More details on the above can be found in the literature (e.g. [28, 33-35]). As lateral spreading is normally assessed as a function of the ground slope and the proximity to a free face [38], LSN is not considered to be representative of liquefaction-induced horizontal displacements.

Table 2: 2011 Christchurch earthquake-based studies that have proposed liquefaction vulnerability parameters-based Repair Rate models. Complete names of the pipe materials are given in the list of acronyms.

Study Reference	Hazard Parameter/s	Earthquakes Causing the Damage	Pipe Diameter (ϕ)	Pipe Materials	Functional Form
[11]	SV1D; LPI; LSN	22 February 2011	75–600 mm	AC, CI, PVC	Linear
[21]	PGV and LSN	22 February 2011	100–600 mm	AC, CI, PVC	Linear
[30]*	LRI	22 February 2011 13 June 2011 23 December 2011	Not specified	AC, CI, PVC, CLS, GI, MDPE and HDPE80	-
[31]	PGV and CRR (at GWD)	22 February 2011 13 June 2011	80–300 mm (AC, CI and PVC); less than 80 mm (GALV, HDPE and MDPE80)	AC, CI, PVC, GI, HDPE, MDPE80	Corrected power
[36]*	LSN	22 February 2011 13 June 2011	Mains (>75 mm)	Ductile and non-ductile	-

**Does not provide Repair Rate models using a functional form. Instead, Repair Rates (or total number of repairs per kilometre) are provided for liquefaction severity index ranges.*

LSN, SV1D and LPI parameters were used by [11] to derive RR models for AC, CI and PVC pipes of diameters ranging from 75 to 600 mm. The models were derived using repair data related to the 22 February 2011 earthquake and the results are presented for the 15th, 50th and 85th percentiles of the CRR. Other studies using LSN data from the Christchurch events are [36] and [37]; the former work includes LSN as an additive factor for PGV-based RR models for AC, CI and PVC pipes with diameters between 100 and 600 mm, and the latter study provides RR (for pipes grouped by diameter and material type) for broad LSN ranges.

As can be seen from Table 2, there is scope for improvement of some of the existing LSN-based RR models and/or gaps in works that can be filled, such as: (1) LSN-based RR models in [11] for AC, CI and PVC pipes are based on data from pipes of diameters between 75 and 600 mm that were exposed to the February 2011 event. Approximately 50% of the total pipe length in the network was represented by pipes of diameter less than 75 mm, and many of those pipes also got damaged in the Christchurch earthquakes ([37]); and (2) Most of the existing models are based on data relating to the February 2011 event only. The use of a combined repair dataset (i.e. from both the 22 February and 13 June 2011 events) gives the opportunity of increasing the exposure length of pipelines of different diameters and materials.

In the present study, we have re-analysed the pipe repair data relating to the Christchurch water supply network that was affected by the 22 February and 13 June 2011 events and derived new LSN-based RR models. Details on these are provided in the following sections.

WATER SUPPLY PIPE NETWORK DATA

Pipe information for the current work utilises the data collected as part of an earlier study [37]. The database included approximately 3,500 km of water pipelines (in total), with pipes made of different materials and of diameters (ϕ) ranging between 20 and 600 mm. Figure 1 shows the total length of the pipeline in the network distributed into pipes grouped by diameter and material ductility type, and Figure 2 shows its geographical distribution. Of the 1,723 km pipes of ϕ <75 mm, about 85% of this pipe length was made of ductile material type (remaining 15% was made up of non-ductile material). The proportion of ductile material pipes in ϕ ≥75 mm group was about 37% (of 1,776 km), with the remainder in this diameter group (i.e. 63%) represented by pipes made of non-ductile material.

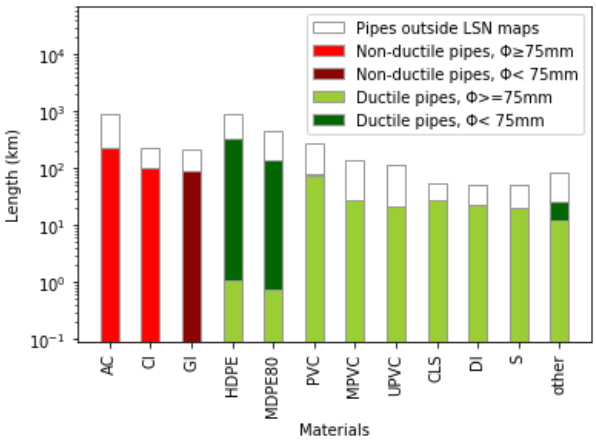

Figure 1: Distribution of the total pipe length in the water network.

Repair data relating to the damaged water pipes in the network was compiled by the Stronger Christchurch Infrastructure Rebuild Team (SCIRT) and provided by Christchurch City Council (CCC) [37]. In general, limited information about the type of repair or cause (e.g. leak or break) was available, but the inspection dates or repair request dates noted by the restoration crews were generally included. This information was helpful to relate an earthquake to an observation of damage and subsequent repair. As suggested in other studies dealing with similar pipe restoration data (e.g. [10,11]), the cumulative number of repairs as a function of time right after the event follow a pattern of an initial high rate of repair, followed by a transient state with an intermediate repair rate and, finally, a steady state of repair with a rate close to the pre-earthquake repair rate (i.e. 'business as usual'). The beginning of the steady state of repair is considered to show when the repair period associated with the event ends. This tri-linear trend was identified in the collected repair data. For the 22 February 2011 earthquake, the change to a steady state of repair was found to occur around 15 April 2011; therefore, repairs identified in the inspection process before 15 April 2011 were considered pipe faults related to the February

earthquake. For the 13 June 2011 event, the onset of transition to the steady state occurred approximately two months after the earthquake (i.e. repairs taken until the 13 August 2011 were considered related to the June event).

LIQUEFACTION SEVERITY NUMBER (LSN) MAPS

As mentioned earlier, the damage to Christchurch's land and built environment was largely caused by permanent ground damage, including liquefaction and lateral spreading in areas close to rivers, wetlands and estuaries. Extensive studies were undertaken following the CES earthquakes to assess the vulnerability of flat land to liquefaction damage and lateral spreading damage (see [28,32-35,39]). LSN maps relating to the 22 February and 13 June 2011 events were produced by Tonkin & Taylor using data from around 15,000 CPT soundings (where 95% of them were deeper than 10 m). The method from [41] was used in the liquefaction potential analysis; the 15th, 50th and 85th percentiles of the CRR were used to calculate the volumetric strain of the soil layers and corresponding LSN values at each site. PGA values recorded for each event and interpolated using the conditional probability interpolation method [41], and ground water level models for the events [28], were used in the calculation. Given that LSN calculations include ground shaking intensities, magnitude and ground water conditions, the expected level of severity for a given LSN value is taken consistent between earthquakes, thus allowing the combination and comparison of damage datasets from different events. The close spacing in time between the 22nd February and the 13th June events could have potentially affected the liquefaction severity due to repeated densification of the soil layers (the volumetric densification under further cyclic shearing should reduce as the material densifies); however, this effect was not considered in the calculation. Due to the even distribution of CPTs in the area, a natural neighbour interpolation process, weighted by distance, was carried out between the CPT sites. The resulting maps, in raster format, had a resolution of 10 m and covered the areas shown in Figure 3a and b for the February and June events, respectively. It should be noted that the LSN maps cover most (but not all) of the areas in the city affected by liquefaction. Only the portion of the network covered by the LSN maps (Figure 3) was used in the RR model development. Also, as noted before, LSN is not representative of lateral spreading effects as this is not sensitive to slope variations or proximity to a free face. Therefore, portions of the network in areas where severe lateral spreading effects was observed [28] are not included in the calculations.

The pipe network was divided into segments and spatially joined to the 50th percentile CRR LSN maps. With this, each segment (having length equal to or less than 20 m to be able to capture the variability in the LSN values across the area) was assigned the LSN value at its location (i.e. centroid of the segment). The repair data were also spatially mapped to the pipe layer; Figure 4 shows the repair distribution of pipes within and outside the LSN map coverage.

The LSN maps covered approximately 34% of pipelines of ϕ <75 mm (i.e. 588 km out of 1,723 km) and 30% of pipelines of $\phi \geq$75 mm (i.e. 532 km out of 1,776 km). For the February event, the LSN map covers about 64% of the repairs made to the pipes of ϕ <75 mm (i.e. 983 out of 1,535 repairs registered in the whole network) and 70% of the repairs registered under pipes of $\phi \geq$75 mm (1050 out of 1,487 repairs in the whole network). For the June event, the LSN map covers 64% of the repairs made to pipes of ϕ <75 mm (i.e. 229 out of 358 repairs in the whole network) and 65% of the repairs registered under pipes of $\phi \geq$75 mm (i.e. 249 out of 383 repairs in the whole network).

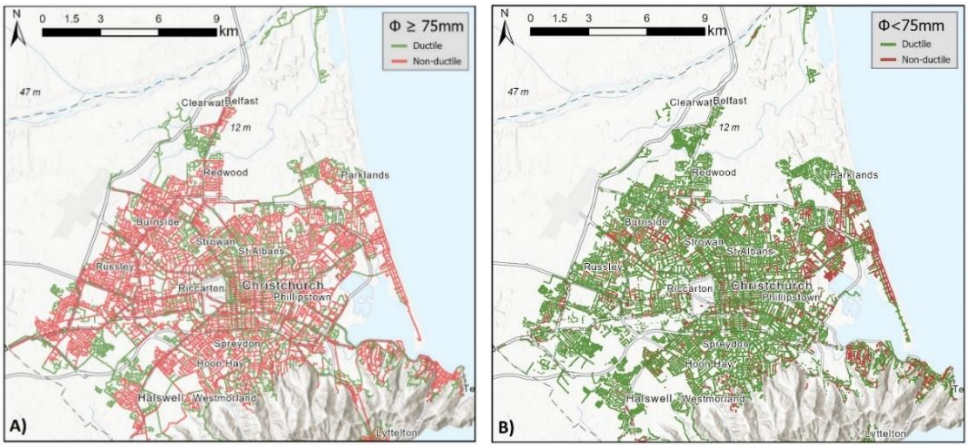

Figure 2: Spatial distribution of ductile and non-ductile pipes of: (a) diameter (ϕ) equal or greater than 75 mm; and (b) diameter (ϕ) less than 75 mm.

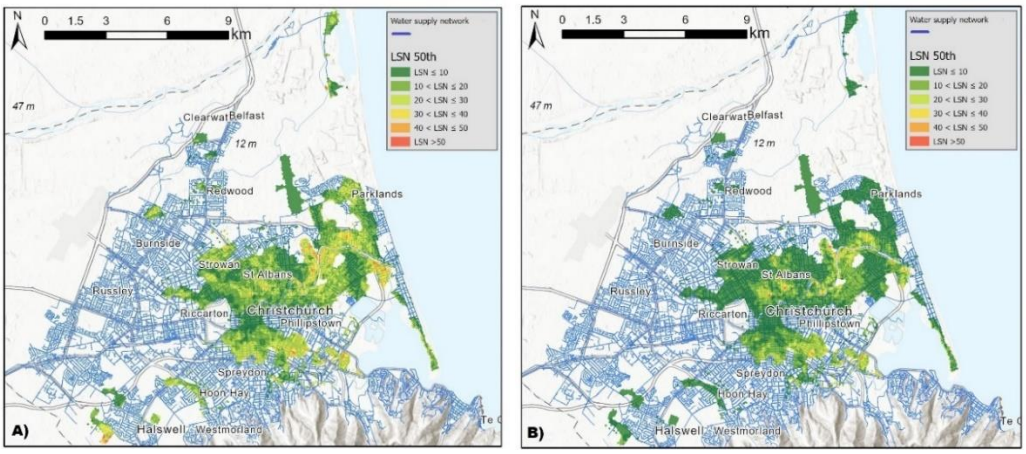

Figure 3: 50th percentile LSN for the 22 February (A) and 13 June (B) 2011 earthquakes.

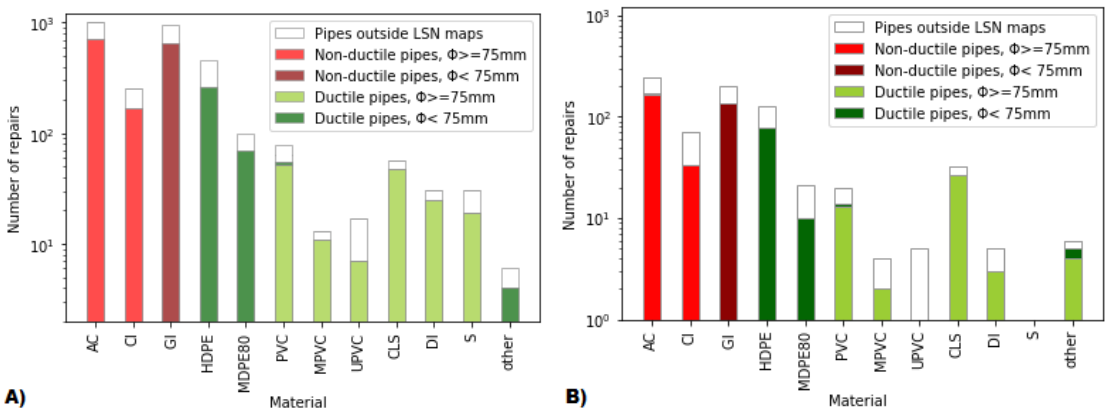

Figure 4: Number of pipe repairs relating to 2011 Christchurch earthquakes: (a) 22 February event; and (b) 13 June event.

Table 3: Repair Rate statistics for water pipes affected during the 22nd February 2011 and 13th June 2011 Christchurch earthquakes.

Material/ Group	Christchurch Water Supply Network			Areas within the LSN Maps			Areas with Liquefaction Observed				Areas with no Liquefaction Observed			
	Length (km)	RR		Length (km)	RR		Length (km)		RR		Length (km)		RR	
	-	Feb	Jun	-	Feb	Jun	Feb	Jun	Feb	Jun	Feb	Jun	Feb	Jun
All	3499	0.88	0.22	1094	1.83	0.43	1084	1050	1.89	0.45	2331	2367	0.39	0.09
Ductile	2074	0.38	0.11	678	0.73	0.21	662	661	0.79	0.21	1411	1416	0.18	0.05
Non-ductile	1130	1.13	0.28	325	2.79	0.65	334	310	2.76	0.64	795	817	0.44	0.13
AC	902	1.13	0.27	225	3.3	0.78	236	223	3.1	0.73	667	678	0.4	0.14
CI	227	1.11	0.31	100	1.67	0.34	98	86	1.94	0.43	129	140	0.47	0.24
PVC	272	0.29	0.07	82	0.66	0.18	81	78	0.69	0.19	191	193	0.11	0.03
HDPE	923	0.49	0.14	339	0.75	0.24	337	330	0.85	0.21	585	593	0.28	0.1
MDPE80	461	0.21	0.05	138	0.51	0.07	133	144	0.54	0.09	328	321	0.09	0.02
GI	211	4.54	0.95	91	7.15	1.49	88	78	7.34	1.77	124	133	1.53	0.47

As damage related to liquefaction is assumed not to occur or is negligible at LSN = 0, only those pipe segments with LSN>0 were considered for RR model development. Within the areas covered by the LSN maps, only 1.5 km of pipes of $\phi \geq 75$ mm was located where LSN = 0; this represents less than 0.3% of the total exposure length in this diameter group (532 km). Similarly, less than 0.3% (1.6 km) of the pipes of $\phi < 75$ mm (exposure length of 588 km) are located where LSN = 0. None of these pipes in LSN = 0 areas suffered damage; the reason for this is deeper ground water levels and more dense soil layers lead to lower or negligible permanent ground deformations.

Table 3 provides a summary of the mean repair rates for pipes damaged in 22nd February and 13th June 2011 Christchurch earthquakes. As expected, the non-ductile group and AC, CI and GI materials show larger RRs than the ductile group and PVC, HDPE and MDPE80. RR values in areas where liquefaction was observed (as reported in [41]), is several times larger than those RR in areas where no liquefaction was observed, and pipe damage can be attributed to transient ground deformations. Similar results have been shown in other studies [10, 11] for the 22nd February 2011 event.

Also, consistent with the larger intensity of the shaking and the consequent increased liquefaction severity, the February event caused more damage to the pipes (resulting in higher repair rate) than the June event, as shown in Table 3.

PIPE FRAGILITY MODEL DEVELOPMENT

The first step for deriving RR models consisted in calculating the mean RR within LSN bins of equal size. In order to remove extreme repair rate that can arise from low sample sizes (i.e. short total lengths), the calculated repair rates were put through a screening criterion (described in [10]). The screening method assumes that the damage data follows a Poisson distribution and defines the minimum sample length required for using the grouped data with a confidence interval of 90% and a standard deviation of 50%. We developed an optimisation algorithm to maximise the number of data points included in each regression. The algorithm iterates through all possible LSN bin sizes and selects the minimum bin size where all of the points pass the screening criteria. Figure 5 shows the RR points for pipes of different materials that passed the screening criteria. The figure shows that the repair rate typically increases with liquefaction severity and that the non-ductile pipes sustained more damage than pipes made of ductile material. In general, the repair rate obtained using the combined dataset (Figure 5a) show lower repair rate than those obtained using the February dataset only (Figure 5b). This should be expected, as repair works following the February event strengthened the network, making it more resistant against the June event.

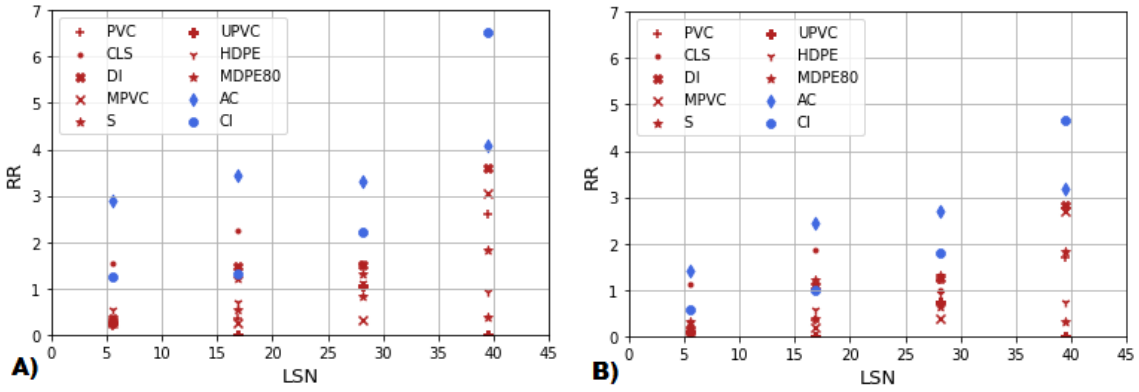

Figure 5: Mean repair rate (i.e. RR = number of pipe repairs/km) from: (a) 22 February event dataset; (b) 22 February and 13 June events combined dataset. Pipes made of ductile and non-ductile material are respectively shown in red and blue.

Table 4: Equation (3) parameter values.

22 February Event Dataset

Diameter (ϕ) Group	Material Group	a_0	b_0	σ_{m0}
ϕ≥75 mm	Generic	1.023	0.049	0.965
	Ductile	-0.020	0.055	0.277
	Non-ductile	2.065	0.044	0.308
ϕ<75 mm	Ductile	0.301	0.023	0.062
	Galvanised Iron	3.950	0.205	0.702

22 February and 11 June Event Combined Dataset

Diameter (ϕ) Group	Material Group	a_0	b_0	σ_{m0}
ϕ≥75 mm	Generic	0.460	0.049	0.637
	Ductile	-0.034	0.044	0.173
	Non-ductile	0.954	0.054	0.192
ϕ<75 mm	Ductile	0.129	0.022	0.153
	Galvanised Iron	1.459	0.233	0.644

Four regression methods (linear, exponential, polynomial and natural log) were explored to fit the RR vs. LSN datapoints. Due to the linear trend observed in the data points, and because the Ordinary Least Squares (OLS) linear fit was found to provide smaller standard deviation on the residuals than other options, the OLS method was chosen to develop the repair rate functions.

As explained earlier, LSN combines the geotechnical characteristics of the soil layers and ground water conditions at a site for a given earthquake shaking and magnitude; similar liquefaction severity (i.e. land damage) is expected at all sites with the same LSN value. Based on this assumption, two sets of RR models were derived in this study: First, using the repair dataset and LSN map associated with the 22 February event, and, second, by combining the datasets from the 22 February and 13 June events. The combined dataset from both earthquake events increased the exposure length, also helped reduce any potential bias from considering only a single event.

For each of the two datasets explained above, two sets of RR models were developed: (a) models based on pipes grouped by diameter and material ductility; and (b) material-specific RR models. Details of these models are explained below.

Repair Rate Models based on Grouped Pipes

Prior to developing RR models for pipes of specific material, RR models were derived based on data from pipes grouped by diameter (i.e. ϕ <75 mm or ϕ ≥75 mm) and material type (i.e. ductile or non-ductile). To avoid those materials with larger total lengths having more weight in the generic equation, these models were derived using weighted mean data pairs calculated for the ductile and non-ductile material groups.

The OLS regression method was used to derive all RR models (Figure 6); the general form of the models is given by Equation 3. Here, parameters a_0 and b_0 and the standard deviation of the residuals (σ_{m0}) for each set of models are provided in Table 4.

$$RR = a_0 + b_0 \, LSN \quad (3)$$

Note that a large proportion of non-ductile pipes of ϕ <75 mm in the network is represented by GI pipes (see Figure 1). These pipes performed poorly during the earthquakes, having repair rate several times the mean repair rate of pipes of other materials (Table 3). Therefore, GI pipes were excluded from the grouping and a separate class was created for them as shown in Figure 6d. Also included in Table 4 and shown in Figure 6 are 'Generic' repair rate models that were derived from combining pipes of all material types in the ϕ ≥75 mm group dataset. These models can be used to estimate RRs in cases where pipe diameter is known but no information on the pipe material is available for damage modelling.

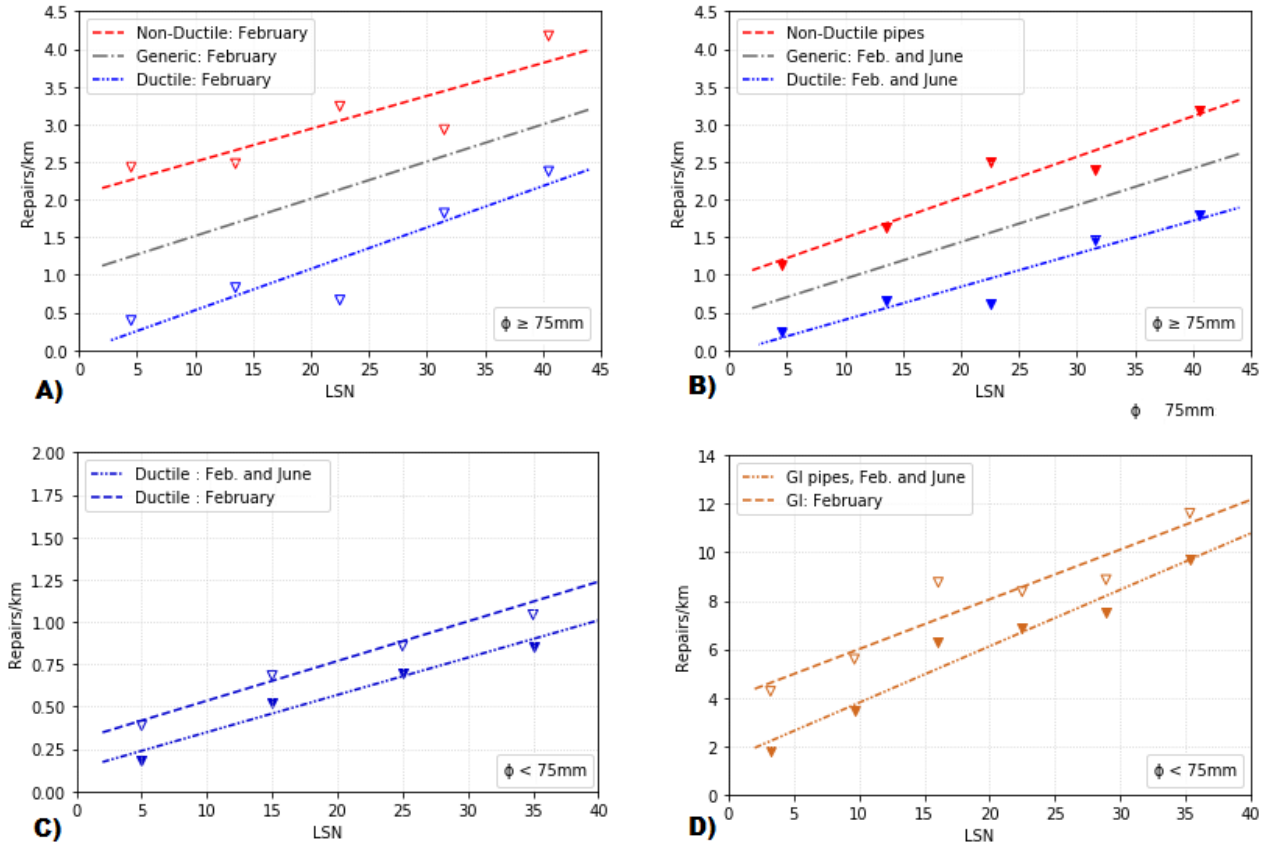

Figure 6: Proposed repair rate (RR) models for: A), B), ductile, non-ductile and generic groups with $\phi \geq 75$ mm derived from the 22 February event dataset and 22 February and 13 June events combined dataset, respectively; C) ductile group with $\phi < 75$ mm for ductile pipes; and D) galvanised iron (GI) pipes with $\phi < 75$ mm. Unfilled triangles represent the data points used for the February event regressions, whereas filled triangles correspond to February and June event combined datasets.

Table 5: Equation (4) parameter values.

22 February Event Dataset

Diameter (ϕ) Group	Pipe Material	a_0	b_0	a_1	b_1	σ_{mc}
$\phi \geq 75$ mm	AC	2.065	0.044	0.764	-0.018	0.303
	CI	2.065	0.044	-1.393	0.023	0.402
	PVC	-0.020	0.055	-0.827	0.046	0.583
$\phi < 75$ mm	HDPE	0.301	0.023	0.028	0.004	0.075
	MDPE80	0.301	0.023	-0.125	-0.004	0.142

22 February and 11 June Event Combined Dataset

Diameter (ϕ) Group	Pipe Material	a_0	b_0	a_1	b_1	σ_{mc}
$\phi \geq 75$ mm	AC	0.954	0.054	0.462	-0.01	0.266
	CI	0.954	0.054	-0.841	0.011	0.230
	PVC	-0.034	0.044	-0.595	0.030	0.322
$\phi < 75$ mm	HDPE	0.129	0.022	0.024	0.004	0.136
	MDPE80	0.129	0.022	-0.122	-0.002	0.058

Material-Specific Repair Rate Models

In order to develop RR models for pipes made of specific material (AC, CI, PVC, HDPE and MDPE80), we derived correction factors by fitting the residuals between the relationships of each material and diameter group and the datapoints for the analysed material type. OLS linear regression was again used in the residuals fit. The screening criterion was again applied here to ensure that the minimum sample size requirement was met.

The general form of material-specific repair rate models is given by Equation 4. Here, a_1 and b_1 are the material-specific correction factors (Table 5), and a_0 and b_0 are the factors from Table 4. The uncertainty of the material-corrected models (σ_{mc}) was obtained by calculating the standard deviation of the

residuals between the corrected models and the data points for pipes of specific material.

$$RR = a_0 + b_0 LSN + a_1 + b_1 LSN \quad (4)$$

Among the non-ductile pipes of ϕ ≥75 mm, AC pipes show the highest repair rate, especially in the lower LSN ranges (see Figure 7). It is shown in previous studies (e.g. [19,38]) that collar joints in AC pipes are particularly sensitive to differential settlements, causing angular distortions. A common failure type in these pipes is cracking at the joints. Compared to AC pipes, the CI pipelines have better resilient joints and pipe body made of increased wall and shell thickness [10] that help restrict damage. The PVC pipes (i.e. of ductile category) of ϕ ≥75 mm performed better (shown by lower RR, see Figure 7a–b) than the AC and CI pipes. This better performance could be attributed to their higher ductility and longer insertion lengths at the joints [11]. The RRs for AC, CI and PVC pipelines converge at high LSN values, suggesting that large deformations affect all materials similarly. The above observation can be seen in results obtained using the February dataset, as well as with RR calculated using the February and June combined dataset.

From the pipe group of ϕ <75 mm and made of ductile material, MDPE80 pipes show the best performance (i.e. lowest RRs; see Figure 7c and 7d), being close to HDPE pipelines at the low LSN range and diverging with increasing LSN values.

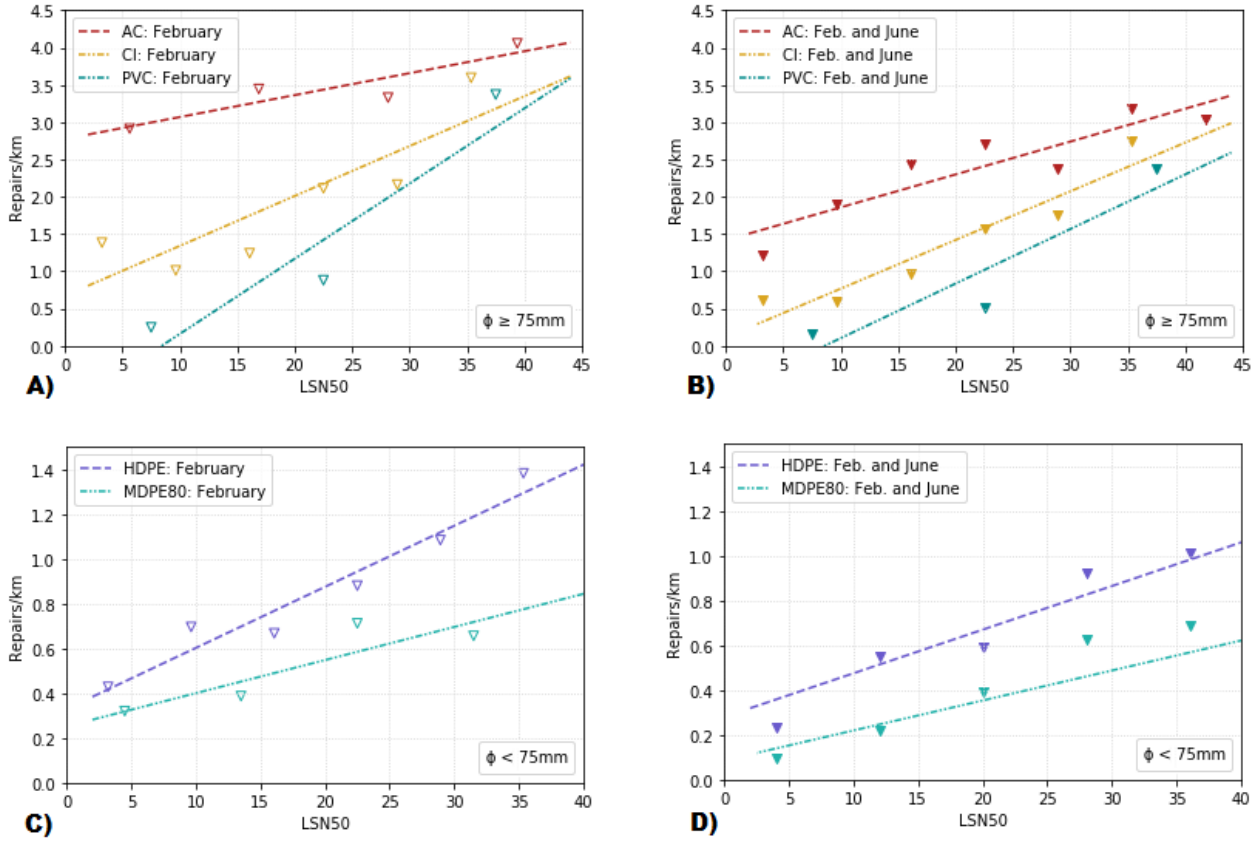

Figure 7: Proposed material-specific RR models for: A), B) AC, CI and PVC pipes with ϕ≥75 mm; C), D) HDPE and MDPE80 pipes with ϕ<75 mm. Datapoints and RR models in A and C correspond to the 22 February event dataset whereas those in B and D correspond to the 22 February and 13 June events combined dataset.

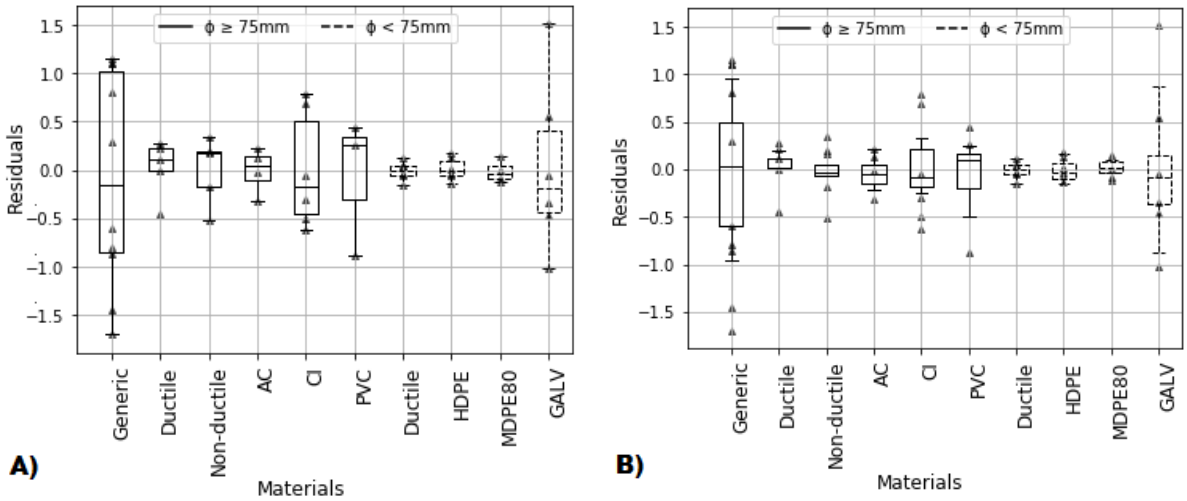

Figure 8: Boxplot of the residuals resulting from each model fit: (a) 22 February event dataset; and (b) 22 February and 13 June event combined dataset.

A boxplot of the residuals for all models derived in this study is shown in Figure 8. It can be observed that the uncertainties are reduced when the February and June event datasets are combined, thereby providing better RR models compared to those based on only the February event dataset.

As summarised in Table 2, a limited number of published studies can be directly compared with the proposed LSN-based RR models proposed in this study; Table 6 shows a comparison between the mean RR given for different LSN ranges in this study and those in [11] and [37]. Normalised residuals between the models presented here and the referenced studies are shown in Figure 9. Models in [11] using the 50th percentile of the CRR show slightly higher RR estimations (i.e. negative residuals) for AC and PVC with a maximum difference in RRs of 16%, whereas CI pipes show lower RR with a maximum difference of 22%. The RR results from models in [37] show larger variability, especially for ductile submains. These lower RR estimations (i.e. positive residuals) should be expected, as the LSN maps in [37] correspond to the 15th percentile of the CRR, whereas the current study used the median CRR based LSN maps.

Table 6: Comparison of mean RR based on models proposed in this study and other published studies: (a) results based on models in [11], (b) results based on models in [37].

a)		**This Study**			**[11]**		
Materials		**AC**	**CI**	**PVC**	**AC**	**CI**	**PVC**
Diameters		**Φ ≥75 mm**	**Φ ≥75 mm**	**Φ ≥75 mm**	**Φ ≥75 mm**	**Φ ≥75 mm**	**Φ ≥75 mm**
LSN Range	0–10	2.5	1.2	-	2.9	1.0	-
	10–20	2.9	1.8	0.6	3.2	1.7	0.7
	20–30	3.3	2.4	1.5	3.5	2.3	1.7
	30–40	3.7	3.0	2.4	3.8	3.0	2.7
	40–50	4.1	3.6	3.3	4.1	3.7	3.7

b)		**This Study**				**[37]**			
Materials		**Ductile**	**Non-ductile**	**Ductile**	**GI**	**Ductile**	**Non-ductile**	**Ductile**	**GI**
Diameters		**Φ ≥75 mm**	**Φ ≥75 mm**	**Φ <75 mm**	**Φ <75 mm**	**Φ ≥75 mm**	**Φ ≥75 mm**	**Φ <75 mm**	**Φ<75 mm**
LSN Range	0–5	0.1	2.2	0.4	4.5	-	2.8	-	-
	5–15	0.5	2.5	0.6	6.0	0.3	1.8	0.5	4.2
	15–25	1.1	2.9	0.8	8.1	0.5	2.4	0.5	6.0
	25–35	1.6	3.4	1.0	10.1	0.6	2.5	0.7	6.4
	35–45	2.2	3.8	1.2	12.2	-	2.3	-	-

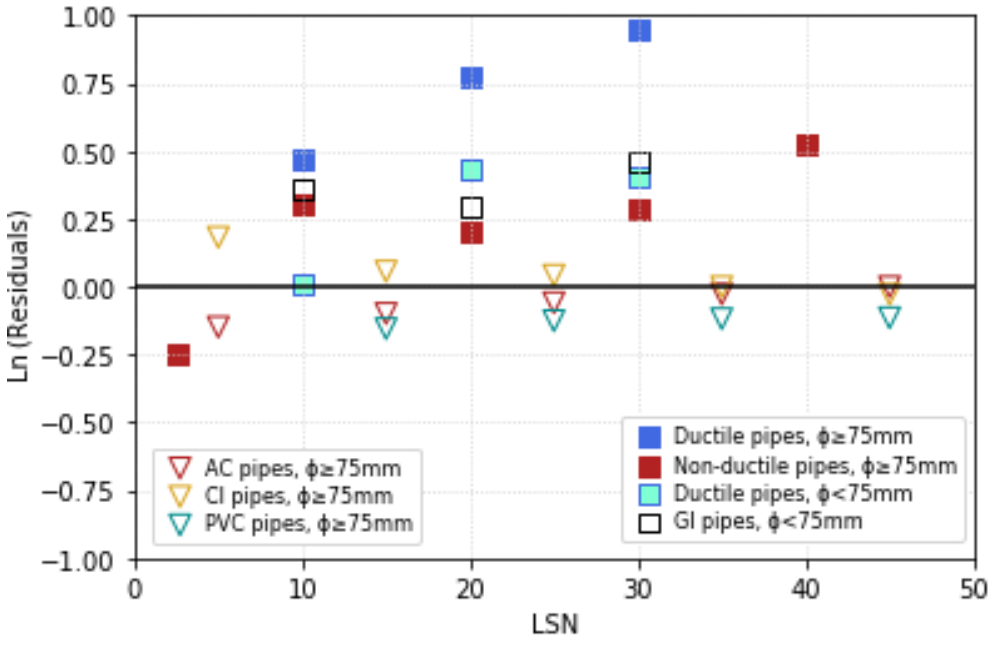

Figure 9: Residuals between RR calculated from models proposed in this study and from [11] (triangles) and [37] (squares).

CONCLUSIONS

The transient and permanent ground deformations generated by the M_W 6.2 22 February and M_W 6.0 13 June 2011 Christchurch earthquakes severely damaged buried water pipes in some areas of the city, resulting in high repair rate (number of repairs per kilometre of pipe exposed to hazard). Most of the damage to pipes was attributed to liquefaction related permanent ground displacement. Pipes made of ductile material (e.g. PVC, HDPE) sustained lesser damage (and therefore resulted in lower repair rate) compared to the pipes made of non-ductile material (e.g. AC, CI). In all cases, the repair rate increased with increasing liquefaction severity.

Utilising the LSN maps and pipe repair data relating to the two events, new repair rate models were developed and presented in this paper. The consistency between LSN calculations between events permitted combining the damage data from February and June, extending the sample length and reducing the uncertainties in the regressions.

Repair Rate functions were derived for pipes grouped by diameter (i.e. ϕ <75 mm or ϕ ≥75 mm) and material type (i.e. ductile or non-ductile). The models were then refined by adding correction factors for those material types with sufficient sample length, enabling material-specific repair rate models to be developed (i.e. for AC, CI and PVC pipes of ϕ ≥75 mm and for MDPE and HDPE80 pipes of ϕ <75 mm). GI pipes performed poorly during the earthquakes, resulting in very high repair rate compared to the other non-ductile pipes of ϕ <75 mm damaged in the network; this warranted a separate repair rate model to be developed for this pipe type.

The proposed repair rate models can be used to estimate the number of pipe repairs on buried water pipes due to potential liquefaction damage from future earthquakes in other urban areas. The input requirements for use of the proposed models are: (1) LSN map for the region of interest [e.g. 42]; and (2) spatial data relating to the water supply pipe network in the region, including pipe diameters and materials. The output produced by using the proposed RR models can provide better understanding of the vulnerability of the pipe network, will help to prioritise resilience investments, contribute to preparing emergency response and recovery plans.

ACKNOWLEDGMENTS

The authors thank Sjoerd van Ballegooy and Virginie Lacrosse of Tonkin & Taylor Ltd for kindly sharing the LSN maps used in this work. The authors are also thankful to their colleagues: Giovanni Pradel, David Heron and Biljana Lukovic for their help with GIS work, and Andrea Wolter and Sheng-Lin Lin for their review comments and suggestions on the paper. Funding support for this work is from GNS Science HRM SSIF Project 1.6: Built Environment and Performance.

REFERENCES

1 Ariman T, Lee B and Chen Q (1987). "Failure of buried pipelines under large ground deformations". *Developments in Geotechnical Engineering*, **49**: 63-75. https://doi.org/10.1016/B978-0-444-98934-5.50010-9

2 Ayala AG and O'Rourke MJ (1989). "*Effects of the 1985 Michoacan Earthquake on Water Systems and other Buried Pipelines in Mexico*". NCEER Technical Report 89-0009, Buffalo, New York, 136 pp. https://www.eng.buffalo.edu/mceer-reports/89/89-0009.pdf

3 O'Rourke T, Stewart HE, Blackburn F and Dickerman TS (1991). "*Geotechnical and Lifeline Aspects of the October 17, 1989 Loma Prieta Earthquake in San Francisco*". NCEER Technical Report 90-0001, Buffalo, New York, 68 pp. https://nehrpsearch.nist.gov/static/files/NSF/PB90208596.pdf

4 Hamada M, Isoyama R and Wakamatsu K (1996). "Liquefaction-induced ground displacement and its related damage to lifeline facilities". *Soils and Foundations*, **36**: 81-97. https://doi.org/10.3208/sandf.36.Special_81

5 Maison B, Lee D, Lau B and Eidinger J (1995). "East Bay Municipal Utility District water distribution damage in 1989 Loma Prieta earthquake". *Proceedings of the Fourth US Conference Sponsored by the Technical Council on Lifeline Earthquake Engineering*, August 10-12, San Francisco, California. 7 pp.

6 Eidinger JM (1998). "*Water-Distribution System*" Page 63-78 in *The Loma Prieta, California, Earthquake of October 17, 1989 – Lifelines*. Editor: Schiff AJ. US Geological Survey Professional Paper 1552-A, Reston, Virginia. https://pubs.usgs.gov/pp/pp1552/pp1552a/pp1552a.pdf

7 Bulletin of the New Zealand Society for Earthquake Engineering, **43**(4). http://www.nzsee.org.nz/bulletin_index/43_4.htm

8 Bulletin of the New Zealand Society for Earthquake Engineering, **44**(4). http://www.nzsee.org.nz/bulletin_index/44_4.htm

9 Cubrinovski M, Hughes M, Bradley B, McCahon I, McDonald Y, Simpson H, Cameron R, Christison M, Henderson B, Orense R and O'Rourke T (2011a). "*Liquefaction Impacts on Pipe Networks. Short Term Recovery Project No. 6*". University of Canterbury Research Report 2011-04, Christchurch, New Zealand, 74 pp. https://ir.canterbury.ac.nz/bitstream/handle/10092/10178/12639392_NHRP-STRP6-Report-v1.0-22DEC11%20with%20Cover.pdf?isAllowed=y&sequence=1

10 O'Rourke TD, Jeon S-S, Toprak S, Cubrinovski M, Hughes M, van Ballegooy S and Bouziou D (2014). "Earthquake response of underground pipeline networks in Christchurch, NZ". *Earthquake Spectra*, **30**(1): 183-204. https://doi.org/10.1193/030413EQS062M

11 Toprak S, Nacaroglu E, van Ballegooy S, Koc AC, Jacka M, Manav Y, Torvelainen E and O'Rourke TD (2019). "Segmented pipeline damage predictions using liquefaction vulnerability parameters". *Soil Dynamics and Earthquake Engineering*, **125**: 105758. https://doi.org/10.1016/j.soildyn.2019.105758

12 van Ballegooy S, Wentz F and Boulanger RW (2015). "Evaluation of CPT-based liquefaction procedures at regional scale". *Soil Dynamics and Earthquake Engineering*, **79**(B): 315-334. https://doi.org/10.1016/j.soildyn.2015.09.016

13 Porter KA, Scawthorn C, Honegger DG, O'Rourke TD and Blackburn F (1992). "*Performance of Water Supply Pipelines in Liquefied Soil*". 16 pp. http://www.sparisk.com/pubs/Porter-1992-water-pipe-liquefied-soil.pdf

14 Pineda-Porras O and Ordaz M (2010). "Seismic fragility formulations for segmented buried pipeline systems including the impact of differential ground subsidence". *Journal of Pipeline Systems Engineering and Practice*, **1**(4): 141-146. https://doi.org/10.1061/(ASCE)PS.1949-1204.0000061

15 Isoyama R, Ishida E, Yune K and Shirozu T (2000). "Seismic damage estimation procedure for water supply pipelines". *Proceedings of the Twelfth World Conference on Earthquake Engineering*, January 30-4 February, Auckland, New Zealand. Paper No 1762. 8 pp. https://www.iitk.ac.in/nicee/wcee/article/1762.pdf

16 Liu X and O'Rourke MJ (1996). "Key parameters for estimating buried pipe damage". *Proceedings of the Eleventh World Conference on Earthquake Engineering*, June 23-28, Acapulco, Mexico. Paper No 1589. 8 pp. https://www.iitk.ac.in/nicee/wcee/article/11_1589.PDF

17 Kuraoka S and Rainer JH (1996). "Damage to water distribution system caused by the 1995 Hyogo-ken Nanbu earthquake". *Canadian Journal of Civil Engineering*, **23**(3): 665-677. https://doi.org/10.1139/l96-882

18 ALA (2001). "*Seismic Fragility Formulations for Water Systems*". American Society of Civil Engineers, Reston, Virginia. 2 vol. https://www.americanlifelinesalliance.com/pdf/Part_1_Guideline.pdf; https://www.americanlifelinesalliance.com/pdf/Part_2_Appendices.pdf

19 ALA (2005). "*Seismic Guidelines for Water Pipelines*". Federal Emergency Management Agency, Washington DC. 39 pp. https://www.americanlifelinesalliance.com/pdf/SeismicGuidelines_WaterPipelines_P1.pdf

20 FEMA. "*HAZUS 2.1 Technical Manual*". Federal Emergency Management Agency, Washington DC. 718 pp. https://www.fema.gov/sites/default/files/2020-09/fema_hazus_earthquake-model_technical-manual_2.1.pdf

21 Bouziou D and O'Rourke TD (2017). "Response of the Christchurch water distribution system to the 22 February 2011 earthquake". *Soil Dynamics and Earthquake Engineering*, **97**: 14-24. https://doi.org/10.1016/j.soildyn.2017.01.035

22 Toprak S, Taskin F and Koc AC (2009). "Prediction of earthquake damage to urban water distribution systems: a case study for Denizli, Turkey". *Bulletin of Engineering Geology and Environment*, **68**: 499. https://doi.org/10.1007/s10064-009-0230-1

23 Robertson PK and Wride CE (1998). "Evaluating cyclic liquefaction potential using the cone penetration test". *Canadian Geotechnical Journal*, **35**(3): 442–459. https://doi.org/10.1139/t98-017

24 Youd TL, Idriss IM, Andrus RD, Arango I, Castro G, Christian JT, Dobry R, Finn WDL, Harder LF, Jr, Hynes ME, Ishihara K, Koester JP, Liao SSC, Marcuson WF, Martin GR, Mitchell JK, Moriwaki Y, Power MS, Robertson PK, Seed RB and Stokoe KH (2001). "Liquefaction resistance of soils: Summary report from the 1996 NCEER and 1998 NCEER/NSF workshops on evaluation of liquefaction resistance of soils". *Journal of Geotechnical and Geoenvironmental Engineering*, **127**(10): 817-833. https://doi.org/10.1061/(ASCE)1090-0241(2001)127:10(817)

25 Boulanger RW and Idriss IM (2014). "*CPT and SPT based Liquefaction Triggering Procedures*". University of California, Department of Civil and Environmental Engineering, Center for Geotechnical Modeling Report UCD/CGM-14/01, Davis, California, 134 pp. https://facultysand.engineering.ucdavis.edu/boulanger/wp-content/uploads/sites/71/2014/09/Boulanger_Idriss_CPT_and_SPT_Liq_triggering_CGM-14-01_20141.pdf

26 Cubrinovski M, Bradley B, Wotherspoon L, De Pascale G and Wells D (2011b). "Geotechnical aspects of the 22 February 2011 Christchurch earthquake". *Bulletin of the New Zealand Society for Earthquake Engineering*, **44**(4): 205-226. https://doi.org/10.5459/bnzsee.44.4.205-226

27 Iwasaki T, Tatsuoka F, Tokida K and Yasuda S (1978). "A practical method for assessing soil liquefaction potential based on case studies at various sites in Japan". *Proceedings of the Second International Conference on Microzonation*, November 26-1 December, San Francisco, California. pp. 885–96.

28 Tonkin & Taylor (2013). "*Liquefaction Vulnerability Study*". Report for the Earthquake Commission, Wellington New Zealand, 50 pp. https://www.eqc.govt.nz/sites/public_files/documents/liquefaction-vulnerability-study-final.pdf

29 Lacrosse V, van Ballegooy S and Bradley BA (2015). "Effect of liquefaction triggering uncertainty on liquefaction consequence". *6th International Conference on Earthquake Geotechnical Engineering*, November 1-4, Christchurch, New Zealand, 9 pp. https://secure.tcc.co.nz/ei/images/ICEGE15%20Papers/Lacrosse_507.00.pdf

30 Cubrinovski M, Hughes M, Bradley B, Noonan J, McNeill S, English G and Sampedro IG (2015). "*Horizontal Infrastructure Performance and Application of the Liquefaction Resistance Index Methodology in Christchurch City through the 2010-2011 Canterbury Earthquake Sequence*". University of Canterbury Research Report 2015-5, Christchurch, New Zealand, 49 pp. https://ir.canterbury.ac.nz/handle/10092/15093

31 Bellagamba X, Bradley BA, Wotherspoon LM and Hughes MW (2019). "Development and validation of fragility functions for buried pipelines based on Canterbury Earthquake sequence data". *Earthquake Spectra*, 35(3): 1061-1086. https://doi.org/10.1193/120917EQS253M

32 van Ballegooy S, Wentz F and Boulanger RW (2015a). "Evaluation of CPT-based liquefaction procedures at regional scale". *Soil Dynamics and Earthquake Engineering*, **79**(B): 315-334. https://doi.org/10.1016/j.soildyn.2015.09.016

33 Tonkin & Taylor (2015a). "*Canterbury Earthquake Sequence: Increased Liquefaction Vulnerability Assessment Methodology*". Report for the Earthquake Commission, Wellington, New Zealand, 185 pp. https://www.eqc.govt.nz/ILV-engineering-assessment-methodology

34 van Ballegooy S, Green RA, Lees J, Wentz F and Maurer BW (2015b). "Assessment of various CPT based liquefaction severity index frameworks relative to the Ishihara (1985) H1-H2 boundary curves". *Soil Dynamics and Earthquake Engineering*, **79**(B): 347-364. https://doi.org/10.1016/j.soildyn.2015.08.015

35 van Ballegooy S, Malan P, Lacrosse V, Jacka ME, Cubrinovski M, Bray JD, O'Rourke TD, Crawford SA and Cowan H (2014). "Assessment of liquefaction-induced land damage for residential Christchurch". *Earthquake Spectra*, **30**(1): 31-55. https://doi.org/10.1193/031813EQS070M

36 Bouziou D, van Ballegooy S, Storie L and O'Rourke TD (2019). "*Spatial Correlations of Underground Pipeline Damage in Christchurch: Correlations with Liquefaction-Induced Ground Surface Deformations and CPT-based Liquefaction Vulnerability Index Parameters*". Report for UC Quake Centre, Christchurch, New Zealand. 50 pp. http://resources.quakecentre.co.nz/wp-content/uploads/2019/09/0806109_FINAL_LiquefactionReport-1.pdf

37 Sadashiva VK, Nayyerloo M and Sherson AK (2019). "*Seismic Performance of Underground Water Pipes during the Canterbury Earthquake Sequence*". GNS Science Consultancy Report 2017/188, Lower Hutt, New Zealand, 64 pp. Prepared for Opus International Consultants Ltd.

38 Zhang G, Robertson PK and Brachman RWI (2004). "Estimating liquefaction-induced lateral displacements using the standard penetration test or cone penetration test". *ASCE Journal of Geotechnical and Geoenvironmental Engineering*, **130**: 861–871. https://doi.org/10.1061/(ASCE)1090-0241(2004)130:8(861)

39 O'Callaghan FW (2014). "Pipeline performance experiences during seismic events in New Zealand over the last 27 years". *Proceedings of the 17th Plastic Pipes Conference*, September 22-24, Chicago, Illinois, USA.

40 Maurer BW, Green RA and Taylor O-DS (2015). "Moving towards an improved index for assessing liquefaction hazard: Lessons from historical data". *Soils and Foundations*, **55**(4): 778-787. https://doi.org/10.1016/j.sandf.2015.06.010

41 Bradley BA and Hughes M (2012). "*Conditional Peak Ground Accelerations in the Canterbury Earthquakes for Conventional Liquefaction Assessment*". Technical Report for the Department of Building and Housing, Wellington, New Zealand, 22 pp.

42 Rosser BJ and Dellow GD (2017). "*Assessment of Liquefaction Risk in the Hawke's Bay. Volume 2: Appendices for Volume 1*". GNS Science Consultancy Report 2015/186, Lower Hutt, New Zealand, 64 pp.

43 Cubrinovski M, Hughes M and O'Rourke TD (2014). "Impacts of liquefaction on the potable water system of Christchurch in the 2010–2011 Canterbury (NZ) earthquakes". *Journal of Water Supply: Research and Technology – Aqua*, **63**(2): 95-105. https://doi.org/10.2166/aqua.2013.004

LIST OF ACRONYMS / SYMBOLS

AC – Asbestos Cement

CI – Cast Iron

CES – Canterbury Earthquake Sequence

CLS – Concrete-Lined Steel

CPT – Cone Penetration Test

CRR – Cyclic Resistance Ratio

DI – Ductile Iron

GI – Galvanised Iron

GWD – Ground Water Depth

HDPE – High-Density Polyethylene

LRI – Liquefaction Resistance Index

LSN – Liquefaction Severity Number

MDPE80 – Medium-Density Polyethylene 80

PGA – Peak Ground Acceleration

PGD – Permanent Ground Displacement

PGV – Peak Ground Velocity

PVC – Polyvinyl Chloride

RI – Riveted Iron

RR – Repair Rate (number of repairs per kilometre)

S – Steel

SV1D – One-Dimensional Volumetric Reconsolidation Settlement

TGD – Transient Ground Deformations

UPVC – Unplasticised Polyvinyl Chloride

WS – Welded Steel

β – Angular Distortion

εHP – Lateral Ground Strains